

Cloud radar Doppler spectra in drizzling stratiform clouds: 2. Observations and microphysical modeling of drizzle evolution

Pavlos Kollias,¹ Wanda Szyrmer,¹ Jasmine Rémillard,¹ and Edward Luke²

Received 24 October 2010; revised 8 March 2011; accepted 16 March 2011; published 2 July 2011.

[1] In part I, the influence of cloud microphysics and dynamics on the shape of cloud radar Doppler spectra in warm stratiform clouds was discussed. The traditional analysis of radar Doppler moments was extended to include skewness and kurtosis as additional descriptors of the Doppler spectrum. Here, a short climatology of observed Doppler spectra moments as a function of the radar reflectivity at continental and maritime ARM sites is presented. The evolution of the Doppler spectra moments is consistent with the onset and growth of drizzle particles and can be used to assist modeling studies of drizzle onset and growth. Time-height radar observations are used to exhibit the coherency of the Doppler spectra shape parameters and demonstrate their potential to improve the interpretation and use of radar observations. In addition, a simplified microphysical approach to modeling the vertical evolution of the drizzle particle size distribution in warm stratiform clouds is described and used to analyze the observations. The formation rate of embryonic drizzle droplets due to the autoconversion process is not calculated explicitly; however, accretion and evaporation processes are explicitly modeled. The microphysical model is used as input to a radar Doppler spectrum forward model, and synthetic radar Doppler spectra moments are generated. Three areas of interest are studied in detail: early drizzle growth near the cloud top, growth by accretion of the well-developed drizzle, and drizzle depletion below the cloud base due to evaporation. The modeling results are in good agreement with the continental and maritime observations. This demonstrates that steady state one-dimensional explicit microphysical models coupled with a forward model and comprehensive radar Doppler spectra observations offer a powerful method to explore the vertical evolution of the drizzle particle size distribution.

Citation: Kollias, P., W. Szyrmer, J. Rémillard, and E. Luke (2011), Cloud radar Doppler spectra in drizzling stratiform clouds: 2. Observations and microphysical modeling of drizzle evolution, *J. Geophys. Res.*, 116, D13203, doi:10.1029/2010JD015238.

1. Introduction

[2] The presence of particle size distributions (PSDs) with separate diameter ranges makes the interpretation of radar observations challenging. The dependency of the backscattering cross section on the sixth moment of the particle diameter often makes the contribution of drizzle particles to the radar observables disproportionate to their contribution to the total particle number concentration and cloud liquid water content. Another impediment in understanding the radar observations is the impact of turbulence that disrupts the correspondence between observed radar Doppler velocity and particle size. These challenges are discussed in detail in part I [Kollias *et al.*, 2011]. New parameters that describe the shape of the radar Doppler spectrum (skewness and kurtosis) were introduced. A comprehensive approach that links radar

Doppler spectrum parameters to cloud microphysics and dynamics was described. Part 1 focused on the application of this new approach in remote sensing of drizzling clouds using profiling millimeter wavelength radars. In particular, a new drizzle detection method was presented based on the presence of positive Doppler spectra skewness values and the use of these new parameters in constraining moment-based retrievals of drizzle parameters was discussed.

[3] Here (part 2), comprehensive profiling cloud radar observations are combined with microphysical modeling to study the onset, growth and depletion of drizzle particles in warm stratiform clouds. Although warm rain microphysics is considered a well-established area of cloud physics [e.g., Stevens *et al.*, 2003; Khairoutdinov and Kogan, 1999], the parameterization of marine stratus clouds in GCMs is a challenge of current concern, particularly due to poor representation of drizzle. Observations [Miller *et al.*, 1998; Albrecht, 1989] and modeling studies [Albrecht, 1993; Lenderink and Siebesma, 2004; Stevens *et al.*, 1998] have shown that drizzle is important principally because it is involved in determining the cloud lifetime and evolution. Along with in situ measurements from microphysical probes, profiling

¹Department of Atmospheric and Oceanic Sciences, McGill University, Montreal, Quebec, Canada.

²Atmospheric Sciences Division, Brookhaven National Laboratory, Upton, New York, USA.

radar Doppler spectra are some of the few available observational methods that provide vertical information on the particle size distribution (PSD). On the modeling side, only explicit bin microphysical schemes provide PSDs, as bulk schemes a priori assume a PSD [e.g., Kogan *et al.*, 1995; Khairoutdinov and Kogan, 1999]. The use of the cloud radar Doppler spectra simulator [Kollias *et al.*, 2011] makes possible the direct comparison between observations and explicit microphysics model output. The use of forward models to bridge the observations has recently received special attention [Klein and Jakob, 1999; Chepfer *et al.*, 2008; Haynes *et al.*, 2007].

[4] The cloud radar observations presented here are from one continental and one maritime site operated by the U.S. Department of Energy (DOE) Atmospheric Radiation Measurement (ARM) Climate Research Facility (described in part 1). The observations are provided in the form of distributions of values of mean Doppler velocity, spectrum width, skewness and kurtosis as a function of the radar reflectivity. In addition, detailed time-height radar observational snapshots are presented to highlight the vertical and horizontal structure of the radar Doppler spectra moments. In parallel, a simple 1-D explicit microphysics model that treats the vertical evolution of drizzle particles in and below the cloud is introduced. The output of the microphysical model is provided as input to the radar Doppler spectra forward model [Kollias *et al.*, 2011] and the output Doppler spectra are used to estimate the radar observables. Using the simulator, many of the observed trends are successfully modeled and interpreted. This includes the early growth of drizzle due to autoconversion and accretion near the top of the cloud layer, and the subsequent growth and then depletion of drizzle particles due to accretion and evaporation respectively during their fall.

2. Observations of Radar Doppler Spectra Moments

[5] Observations from a continental (SGP: Southern Great Plains) and a maritime (Graciosa Island) ARM sites were used to develop a short climatology of observed cloud radar Doppler spectra moments in low stratiform clouds. The continental data set is from a 35 GHz Doppler cloud radar (MMCR: Millimeter-wavelength Cloud Radar) and the maritime data set from a 95 GHz Doppler cloud radar (WACR: W band ARM Cloud Radar). The operational settings of the radars (described in part 1) are very similar. Measurements from a collocated ceilometer and/or micro-pulse lidar were used to estimate the cloud base height and only the radar Doppler spectra above the cloud base (e.g., cloud droplets are always present) are considered for the climatology (Figure 1). The continental cases were observed between May 2006 and January 2007, while the maritime ones were taken from May 2009 to February 2010. Single cloud layer cases were selected with and without drizzle particles below the cloud base. The temperature within the cloud was required to be above the freezing level to discard any possible ice process. Finally, a cloud mask was used in the SGP data set to get rid of any clutter that could have contaminated the data (e.g., insects). A total of 1.36 and 0.66 million recorded radar Doppler spectra were used to develop the maritime and continental climatology respectively.

[6] The distributions of the observed mean Doppler velocity, spectrum width, skewness and kurtosis of the radar Doppler spectra as a function of the observed radar reflectivity at both sites are shown in Figure 1. The choice of radar reflectivity for this coordinate is based on its frequent use as a measure of whether large particles are present in the radar sampling volume. Although the observations are collected over a wide range of atmospheric conditions, the distributions exhibit systematic variability and trends. The most noticeable feature is a narrow radar reflectivity regime that signals the transition from the low radar reflectivity returns of radar Doppler moments dominated by turbulence contributions, to higher radar reflectivity returns where drizzle particle growth processes also contribute to the observed variability [e.g., Kollias *et al.*, 2011]. Starting with the mean Doppler velocity (Figure 1a), at low radar reflectivities, the mean Doppler velocity exhibits a distribution with a near-zero mean. The dominant contribution to this part of the distribution is the radar sampling volume-average vertical air motion. The near-zero mean illustrates the lack of preference in updraft/down-draft vertical air motion and the width of the distribution can be used to infer the turbulence intensity in stratiform clouds [e.g., Kollias and Albrecht, 2000]. At higher reflectivities, the mean Doppler velocity distributions shift toward positive (downward) values indicating the downward bias introduced by the drizzle particles' terminal velocity. The maritime data set exhibits higher mean Doppler velocity values for the same reflectivity range, illuminating the presence of larger drizzle droplets in maritime stratiform clouds. Noticeably, at the -16 dBZ to -4 dBZ regime, continental clouds have higher mean fall velocity than their maritime counterparts (Figure 1a, right). This is mainly caused by few observations with very large values of Doppler velocity and the spectrum width (Figure 1a, left and Figure 1b, left), absent in the maritime cases. The median value of velocity in this reflectivity regime remains however lower in continental than in maritime clouds, except between -17 and -14 dBZ. The transition regime from cloud dominated to drizzle dominated regime is sharper in the continental data set. The reflectivity value where the transition occurs is likely influenced by the cloud droplets' number concentration [Liu *et al.*, 2008], variations in which would have greater impact in the maritime environment, as it is generally characterized by smaller number concentrations. This is also supported by the fact that the continental transition occurs at a higher reflectivity range (from -20 to -15 dBZ) than the maritime (between -30 and -20 dBZ).

[7] A similar transition is observed in the distribution of the Doppler spectrum width as a function of the radar reflectivity for the continental clouds. At low radar reflectivities (below -20 dBZ), the Doppler spectrum width is invariant with radar reflectivity (~ 0.15 ms^{-1}). In this regime, turbulent contributions to the observed spectrum width dominate through the turbulence broadening term (dependency on the turbulent dissipation rate). At the very low radar reflectivities (close to -40 dBZ), the poor signal-to-noise conditions are biasing the estimates of the spectrum width. Such a feature is not observed in the corresponding maritime distribution of spectrum width observations since the WACR is more sensitive than the MMCR. At higher radar reflectivities (-20 to -15 dBZ), the spectrum width "jumps" to a higher value (~ 0.25 ms^{-1}). This indicates the increasing

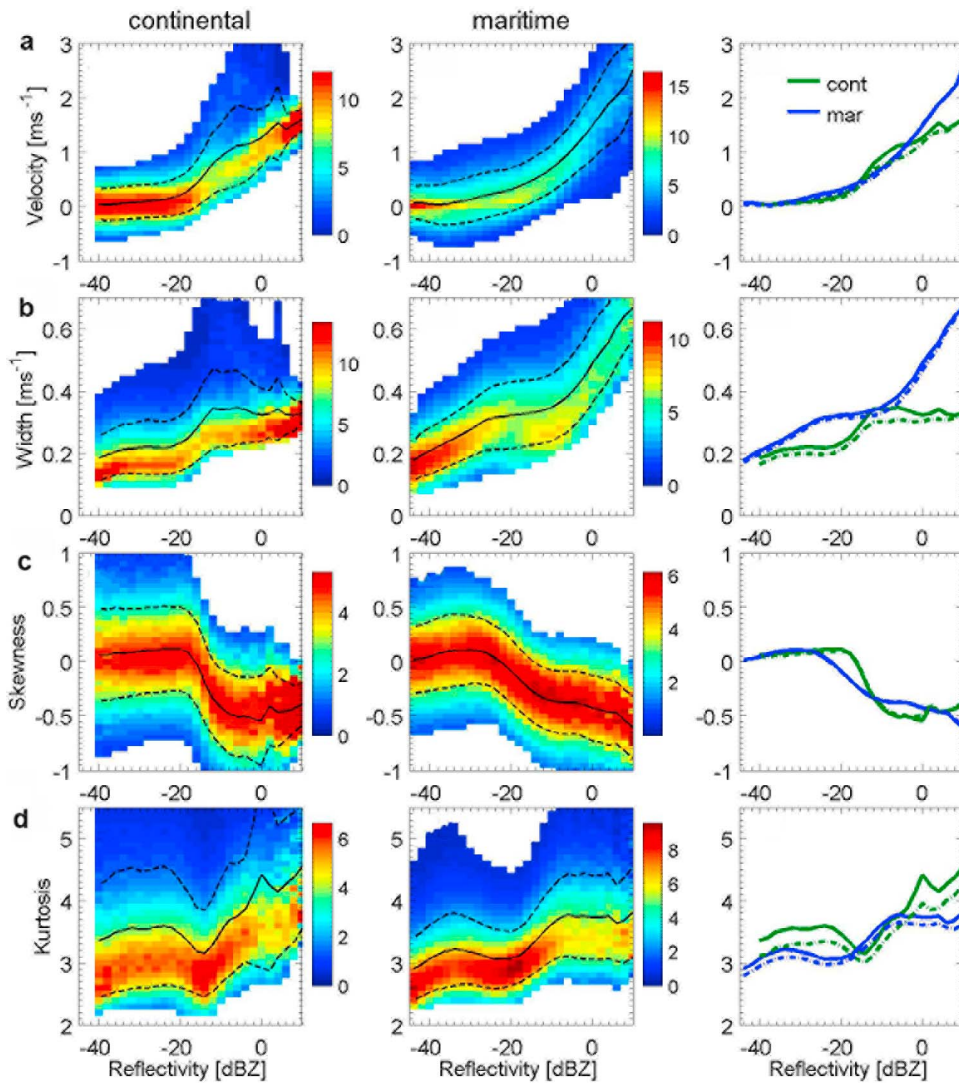


Figure 1. Distribution of the observed radar Doppler spectra parameters ((a) mean Doppler velocity, (b) spectral width, (c) skewness, and (d) kurtosis) as a function of the radar reflectivity. Shown are distributions from inside (left) continental and (middle) maritime stratocumulus clouds. The colors represent the percentage of the data found in each reflectivity bin (2 dBZ wide), while the black lines correspond to the mean (solid line) and standard deviation (dashed line) of the distributions. (right) Comparison of the mean (solid lines) and median (dash-dotted lines) of the continental (green lines) and maritime (blue lines) distributions.

contribution of PSD broadening to the observed Doppler spectrum width values due to drizzle growth. At even higher radar reflectivities, the spectrum width continues to slowly increase. The maritime distributions of Doppler spectrum width have several distinct differences compared to their continental counterparts. A steady increase of the Doppler spectrum width (from 0.15 to 0.3 ms^{-1}) is observed at low radar reflectivities. Since there is no reason to expect a systematic increase of in-cloud turbulence with radar reflectivity, the observed increase is attributed to microphysical factors. It clearly indicates that drizzle particles exist in maritime clouds at very low reflectivities. Another interesting feature is the differing tendencies in the maritime and continental clouds within the reflectivity regime higher than about 0 dBZ. While the average spectrum width in the continental clouds remains

almost constant, in the maritime clouds the observations show a significant increase of the spectrum width with reflectivity. This discrepancy will be examined using modeling in section 4.2.

[8] The distribution of the skewness of the radar Doppler spectrum as a function of the radar reflectivity for continental clouds is also marked by a very sharp transition between -15 to -20 dBZ. At very low radar reflectivity values the skewness is near zero with a very small positive bias. Small-scale turbulence dominated radar Doppler spectra will have a symmetric shape (zero skewness); however under minimal turbulence conditions a small positive skewness bias can be observed [Kollias *et al.*, 2011]. From -40 dBZ to the very sharp transition regime (-20 to -15 dBZ) the skewness increases little with radar reflectivity. This is consistent

with the early growth of drizzle particles because these drizzle particles do not have the size or fall velocity to induce large changes in the Doppler spectra skewness. In the transition regime, the skewness sharply becomes negative and remains negative for higher radar reflectivity values. This is consistent with the presence of a drizzle spectral peak that is higher than the cloud spectral peak. The maritime skewness distributions exhibit similar tendencies as a function of the radar reflectivity; however, there are two differences. In the low radar reflectivity regime (below -20 dBZ), the skewness increase is more noticeable than in the continental case. This is consistent with early growth of drizzle particles that have sizes large enough to impact the skewness of the Doppler spectrum. This observational feature will be examined using modeling in section 4.1. It is plausible that different aerosol loading conditions are responsible for the observed skewness differences in the continental and maritime clouds. Furthermore, in the transition regime, the change in sign of the skewness (from positive to negative) is smoother and occurs over a larger radar reflectivity range.

[9] Finally, the distribution of the kurtosis of the radar Doppler spectrum as a function of the radar reflectivity is shown in Figure 1d. In the transition regime (-25 to -20 dBZ and -20 to -15 dBZ for the maritime and continental clouds correspondingly), the kurtosis develops a local minimum that is consistent with the presence of relatively flat (wide) radar Doppler spectra. Flat radar Doppler spectra can be induced by the relatively equivalent contributions from the cloud and drizzle PSD. At radar reflectivity values lower than the transition regime, the kurtosis exhibits a local maximum with relatively peaked Doppler spectra. This is consistent with the increase in the spectral density of the cloud peak due to condensational growth. At radar reflectivity values higher than the transition regime, kurtosis acquires higher values driven by drizzle particle growth.

[10] Time-height cloud radar observations of a drizzling marine stratus cloud observed by the WACR at the ARM Mobile Facility Graciosa site are provided in Figure 2. A 30 s low-pass filter has been applied to the high-resolution radar measurements to remove the (zero mean) influence of small-scale wind shear across the radar sampling volume on the radar Doppler moments. Measurements from a collocated ceilometer and/or micropulse lidar are used to estimate the cloud base height (black line in Figure 2). The observations cover 72 min of nighttime observations. The laser-detected cloud base and the radar-detected cloud top define the cloud layer, and its average cloud thickness is 250–300 m. During the strong drizzle episode (3.5–4.1 UTC), the maximum radar reflectivity is observed in the middle and lower part of the cloud layer, consistent with drizzle growth. Below the cloud base, a deep virga layer is observed with strong evaporation as indicated by the weakening of the drizzle radar reflectivity toward the surface. The Doppler velocity observations also indicate stronger fall velocities (positive) at the middle and lower part of the cloud layer. Below the cloud base, the height-averaged Doppler velocity decreases; however, the turbulence contribution makes the interpretation challenging.

[11] The same statement is valid for the spectrum width observations. Above the cloud base, higher spectrum width values are observed; however, high spectrum width values do not always coincide with high reflectivity values. This

indicates the strong contribution of turbulence on the observed spectrum width values. The last two panels show the time-height mapping of Doppler spectra skewness and kurtosis. Turbulence within the radar sampling volume acts to shift skewness values to zero and kurtosis values to a value of three. However, in Figure 1, it was illustrated that skewness and kurtosis maintain important information about cloud microphysics. A noticeable feature of the Doppler spectra skewness is the presence of positive values near the cloud top. This is consistent with the development of a drizzle Doppler spectral “tail” and consistent with drizzle onset via the autoconversion process and its early growth by cloud accretion. Lower in the cloud layer, a sharp shift to negative skewness values is observed. This is consistent with Doppler spectra where the cloud radar reflectivity is less than the drizzle radar reflectivity. This extends below the cloud base and finally the evaporation process shifts the Doppler spectra skewness to zero and positive values. The impact of evaporation on radar observations will be examined in section 4.3. The kurtosis of the Doppler spectrum exhibits a local minimum near the middle of the cloud. This is consistent with the presence of a kurtosis minimum in the radar reflectivity transition zone.

[12] Time-height cloud radar observations of a drizzling continental stratus cloud observed by the MMCR at the ARM SGP site are provided in Figure 3. A 30 s low-pass filter has been applied to the high-resolution radar measurements to remove the (zero mean) influence of small-scale wind shear across the radar sampling volume on the radar Doppler moments. The observations cover 66 nighttime minutes. The laser-detected cloud base and the radar-detected cloud top define the cloud layer and its average cloud thickness is 400 m. At the beginning of the observing period (5.4–5.8 UTC), light drizzle is observed, as indicated by the radar reflectivity echoes below the cloud base. The drizzle reflectivity values below the cloud base are low (-35 to -45 dBZ) indicating small diameter drizzle particles. This is consistent with the radar reflectivity maximum near the cloud top, resulting from the cloud PSD profile dominating the radar reflectivity profile. In the absence of the virga echoes, it is difficult to infer the presence of drizzle particles in the cloud layer from the observed radar reflectivity values alone. The time-height mapping of the Doppler velocity and spectrum width provides supporting information for the presence of drizzle in the cloud layer. Higher positive (downward) Doppler velocities are observed near the cloud base along with higher spectrum width values. Similarly, as we observed in the maritime case, high spectrum width values do not always coincide with high reflectivity values. The skewness of the radar Doppler spectrum is very close to zero, indicating cloud dominated Doppler spectra [Kollias *et al.*, 2011]. Localized areas (pockets) of positive skewness are found that coincide with drizzle virga below the cloud base. This suggests that skewness is a very powerful indicator of early drizzle particle growth [Kollias *et al.*, 2011]. Finally, the kurtosis of the radar Doppler spectra on average exhibits values higher than 3. A layer of lower kurtosis values is observed 100–150 m below the cloud top.

[13] The analysis of profiling cloud radar observations of drizzling clouds has identified several noticeable features. These include: (1) the evolution of Doppler spectra moments during early drizzle production near the cloud top and

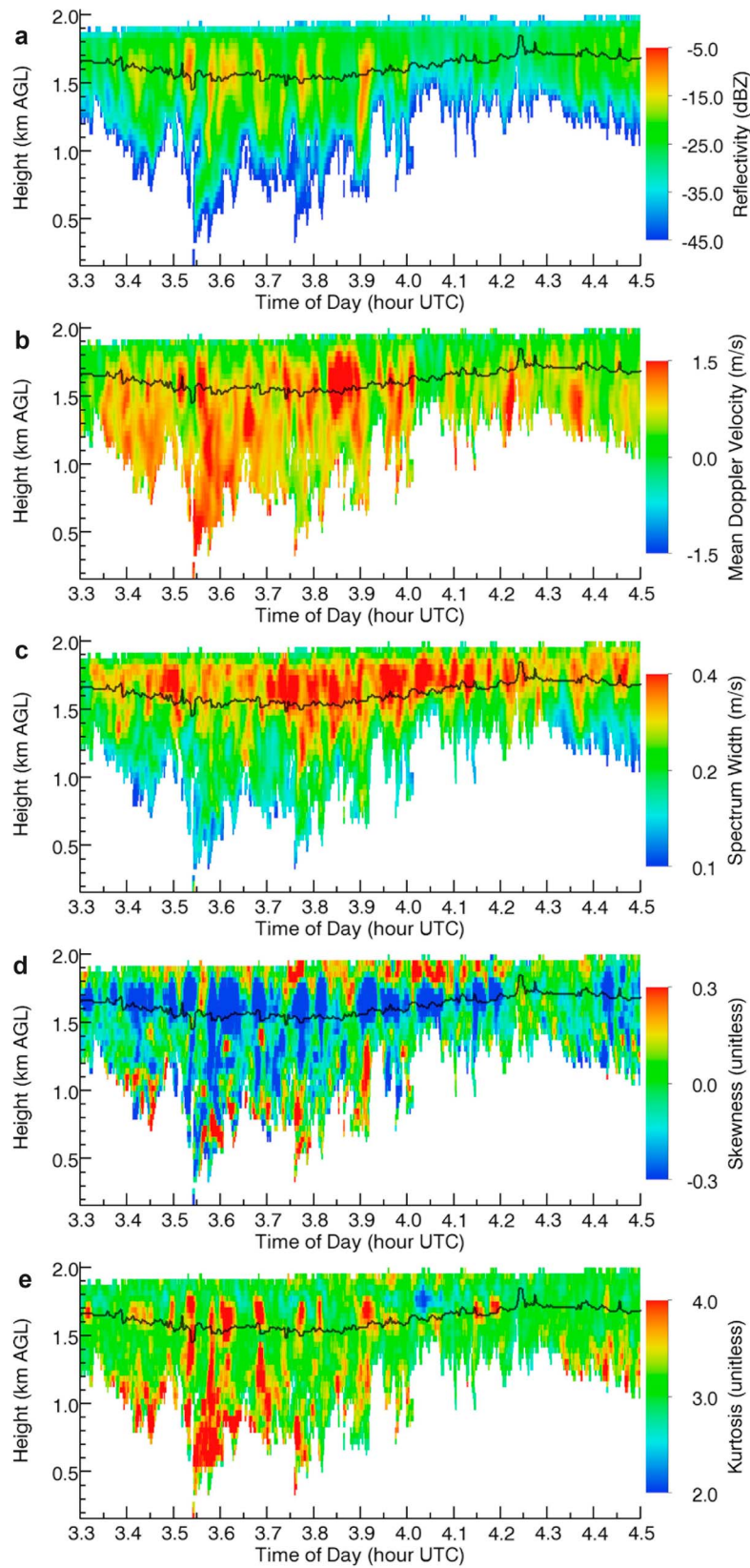


Figure 2. W band radar Doppler spectra moments: (a) reflectivity, (b) mean Doppler velocity, (c) spectral width, (d) skewness, and (e) kurtosis at the ARM AMF Graciosa site during a 72 min period collected on 29 November 2009. The black line represents the corresponding cloud base as detected by a collocated Vaisala ceilometer.

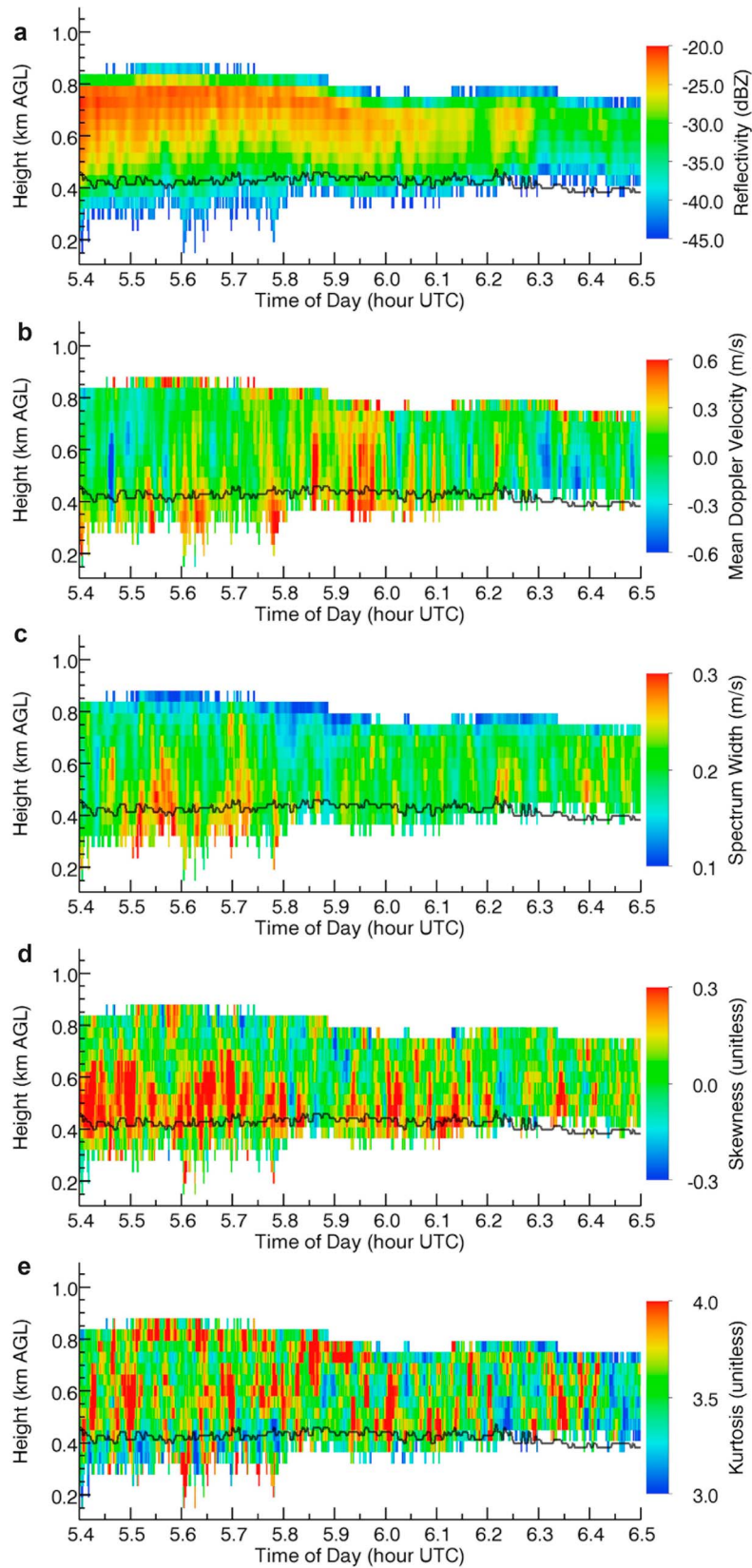


Figure 3. K band radar Doppler spectra moments: (a) reflectivity, (b) mean Doppler velocity, (c) spectral width, (d) skewness, and (e) kurtosis at the ARM SGP site during a 66 min period collected on 28 March 2008. The black line represents the corresponding cloud base as detected by a collocated Vaisala ceilometer.

subsequent growth in the cloud layer, (2) the observed differences in continental and maritime Doppler spectra moments, and (3) the evolution of the Doppler spectra moments below the cloud base under the action of evaporation. These features will be examined in sections 3 and 4 with a simplified modeling approach used to describe microphysical processes in low stratiform clouds.

3. General Description of the Simplified Approach Used to Model Microphysical Processes in Low Stratiform Liquid Clouds

[14] The evolution of the drizzle PSD spectral mode within a cloud layer is represented by its decomposition into individual spectra originating from the autoconversion process at different levels. With some simplifying assumptions about the microphysical growth processes, the approximate evolution of an individual drizzle spectrum as a function of distance fallen is obtained from a general equation describing spectrum development under steady state conditions. The initial input spectrum is prescribed. The spectrum development equation is also used to simulate the effects of evaporation on the drizzle PSD in the subcloud layer.

[15] In our simplified approach, the formation rate of embryonic drizzle droplets via the autoconversion process is not calculated explicitly. The shape of the initial drizzle distribution is prescribed, but its total number concentration is estimated from the formation rate of embryonic drizzle that is parameterized as a function of the assumed cloud droplet number concentration and LWC profile at/above a level at which the spectrum is introduced.

3.1. Description of the Vertical Evolution of an Individual Drizzle Spectrum

[16] Starting from a specified drizzle spectrum at a level z_0 , its evolution in steady state conditions follows this general relation:

$$\frac{\partial}{\partial r} \left(n_d \frac{dr}{dt} \right) + \frac{\partial}{\partial z} \left(n_d \frac{dz}{dt} \right) = 0,$$

where $n_d(r, z)$ represents the drizzle droplet size distribution. This relation neglects the introduction of new droplets by autoconversion, self-collection, breakup and complete evaporation below the cloud base [Gossard *et al.*, 1990; Rogers *et al.*, 1991]. The assumption that droplets fall vertically at their terminal velocity (no vertical and horizontal air motion) leads to $dz/dt = V_f$, with z oriented downward. The air density correction term for fall speed is not taken into account. The expansion of the last relation gives the following partial differential equation:

$$\left. \frac{dr}{dt} \right|_{PRC} \frac{\partial n_d}{\partial r} + V_f \frac{\partial n_d}{\partial z} = -n_d \left[\left. \frac{\partial}{\partial r} \frac{dr}{dt} \right|_{PRC} + \frac{1}{V_f} \left. \frac{dV_f}{dr} \frac{dr}{dt} \right|_{PRC} \right]. \quad (1)$$

The term $\left. \frac{dr}{dt} \right|_{PRC}$, describing the growth rate of the droplets due to microphysical processes at a given level z , can be approximated for a given process PRC by a power law:

$$\left. \frac{dr}{dt} \right|_{PRC} = A(z)r^B. \quad (2)$$

The analytical solution of (1) is obtained assuming that, in a given layer, the evolution of the drizzle spectrum is mainly through one microphysical process described by a unique relation (2), and with the sedimentation parameterized by a unique prescribed power law velocity-size relationship applied for an entire subrange of sizes of interest

$$V_f = \alpha r^\beta. \quad (3)$$

The solution of (1) describing the approximate drizzle PSD as a function of distance fallen $z - z_0$ is obtained in the following form:

$$n_d(r, z) = f_{r,z}^{\beta+B} n_0(f_{r,z} \cdot r, z_0), \quad (4)$$

with

$$f_{r,z} = f_{r,z}(r, \Omega, B, \alpha, \beta) = \left[1 + \frac{B - \beta - 1}{\alpha} \Omega r^{B-\beta-1} \right]^{-1/(B-\beta-1)}, \quad (5)$$

where $n_0(r, z_0)$ is an initial spectrum at the initial level z_0 and $\Omega \equiv \int_{z_0}^z A(z)dz$ is the vertically integrated value of A introduced in (2).

[17] The relation (4) shows that the PSD at a level z can be described by the initial distribution at z_0 displaced along the radius axis by an amount $\Delta r = r(f_{r,z} - 1)$, which is a function of radius and the $f_{r,z}$ term. Moreover, the number concentration changes by a multiplication factor of $f_{r,z}^{\beta+B}$. The input PSD spectra $n_0(r, z_0)$ are assumed to take the form of an analytical function such as lognormal or generalized gamma distributions.

3.2. Parameterization of Microphysical Processes

3.2.1. Growth by Accretion

[18] The drizzle starts when a few cloud droplets traverse the gap between the cloud size regime, dominated by the condensational growth, and the drizzle regime, dominated by growth via the cloud droplet collection process called accretion ACC .

[19] The growth by accretion of a droplet of radius r collecting cloud droplets (r') with volume $v(r')$ is given by:

$$\left. \frac{dr}{dt} \right|_{ACC} = \frac{1}{4\pi r^2} \int_{r_{min}}^{r_{max}} K(r, r') v(r') n(r') dr', \quad (6)$$

where $K(r, r')$ denotes the collection kernel. At the first stage of collectional growth, the small drizzle embryos grow by collection of cloud droplets with a rate that is very small. However, this rate increases rapidly with size due to the increasing collection efficiency. When the drizzle droplets attain 50–60 μm in radius, the collection efficiency becomes mostly size-independent and cloud accretional growth becomes a continuous collection process. To parameterize the collection process, several forms of the kernel function in (6) have been proposed. An approximate form, mathematically simple, is the one derived by Long [1974] describing

the kernel dependence on size with the division between the two regimes taken at $50 \mu\text{m}$:

$$K(r, r') \approx a_{\kappa} r^{3\kappa} \quad (7)$$

$$r = r_{\text{small}} < 50 \mu\text{m} \quad : \quad \kappa = \kappa_1 = 2, \quad a_{\kappa_1} = 1.93 \cdot 10^{17} \text{m}^{-3} \text{s}^{-1} \quad (7')$$

$$r = r_{\text{large}} \geq 50 \mu\text{m} \quad : \quad \kappa = \kappa_2 = 1, \quad a_{\kappa_2} = 2.65 \cdot 10^4 \text{s}^{-1} \quad (7'')$$

Using Long's kernel we obtain from (6):

$$r = r_{\text{small}} < 50 \mu\text{m} \quad : \quad \left. \frac{dr}{dt} \right|_{\text{ACC1}} \approx \frac{a_{\kappa_1}}{4\pi\rho_w} r^4 LWC = C_1 LWC r^4 \quad (8a)$$

$$r = r_{\text{large}} \geq 50 \mu\text{m} \quad : \quad \left. \frac{dr}{dt} \right|_{\text{ACC2}} \approx \frac{a_{\kappa_2}}{4\pi\rho_w} r LWC = C_2 LWC r \quad (8b)$$

where LWC denotes cloud liquid water content: $LWC = \rho_w \int_{r'_{\text{min}}}^{r'_{\text{max}}} v(r') n(r') dr'$ with ρ_w liquid water density. Therefore, the application of Long's kernel introduces the threshold behavior of the accretion process with two stages of drizzle growth. The accretion process for very small drizzle droplets, given in (8a) and hereinafter referred to as ACC1, describes the growth of drizzle embryos freshly transferred from the cloud to the drizzle category. This drizzle regime is similar to the so-called "large-cloud-droplet mode" in the bulk parameterization of *Saleeby and Cotton* [2004]. The second drizzle growth regime, given in (8b) and hereinafter referred to as ACC2, represents continuous accretional growth and relates to the larger drizzle droplets. These larger drops are present at more considerable distances from the level of their generation via autoconversion and falling out of the cloud base through subsaturated air.

[20] This distinction between two regimes with respect to cloud accretion by drizzle is also maintained with respect to the velocity power law (3). In general, the terminal velocity for droplets smaller than about $30 \mu\text{m}$ in radius is represented by (3) with $\beta = 2$ (the Stokes regime), while the value of β progressively decreases for larger droplets, becoming close to 1 for r around $60\text{--}80 \mu\text{m}$. For example, the average relation suggested by *Comstock et al.* [2004] uses $\beta = 1.4$. Here, two different power law relationships for terminal velocity are used which better approximate separately the very small drizzle droplet regime (ACC1: $\alpha = 7.637 \cdot 10^5 \text{m}^{-0.5} \text{s}^{-1}$, $\beta = 1.5$) and the one for larger drops (ACC2: $\alpha = 4.538 \cdot 10^4 \text{m}^{-0.2} \text{s}^{-1}$, $\beta = 1.2$). This artificial separation of the accretion process in two distinct regimes, each with unique power law relationships for accretional growth and terminal velocity, allows the use of the solution (4) with (5) in the analytical study of the drizzle spectrum evolution when controlled mainly by one of the two regimes.

[21] Therefore, the first stage of the evolution of the newly formed drizzle spectrum can be approximately described using (4) with (5), with the parameters $A(z)$ and B from

(2) replaced with the terms from (8a), i.e., $A(z) = C_1 LWC(z)$, leading to $\Omega = C_1 LWP$ (where LWP is the liquid water path in the layer $z_0 - z$), and $B = 4$. Then from (5), the spectrum at a level z located at a small distance below the initiation level z_0 is obtained from the initial spectrum with

$$f_{r,z} = \left[1 + \frac{3-\beta}{\alpha} \Omega r^{3-\beta} \right]^{-1/(3-\beta)}. \quad (9)$$

Since the droplet sizes corresponding to the ACC1 are not very far from the Stokes regime, the exponent of the velocity power law can be put in the form $\beta = 2 - \delta$, with δ positive, but less than 1. This leads to the following approximation: $f_{r,z} \approx 1 - (1/\alpha)\Omega r^{1+\delta}$. Then, the spectrum at z represents the initial spectrum displaced by $\Delta r \approx -(1/\alpha)\Omega r^{2+\delta}$ and multiplied by the factor $f_{r,z}^{6-\delta} \approx 1 - [(6-\delta)/\alpha]\Omega r^{1+\delta}$. Consequently, for small Ω , only a very tiny change with respect to the initial spectrum is expected for the small r considered ($\Delta r \rightarrow 0$, $f_{r,z}^{6-\delta} \rightarrow 1$), resulting from a very slow growth by accretion at these sizes. However, the spectrum modification increases relatively rapidly with increasing r as we can expect from rapidly rising collection efficiency and velocity. It leads to a broadening of the spectrum due to a progressive advancement of the larger droplet tail toward increasing r .

[22] Some error in our modeling of the drizzle evolution under the growth regime ACC1 is introduced due to: (1) the neglecting of the effects of the growth by condensation, which may have some small impact on the evolution of the smaller droplet tail; (2) the assumption about zero air motion; and (3) the neglecting of a turbulence effect. For the larger drizzle droplets growing under the ACC2 regime, the error introduced by these three factors is expected to be much smaller.

[23] A different evolution of the individual drizzle PSD is expected for drizzle that is already developed and grows by a continuous cloud accretion ACC2. From (8b), this growth process is described by the parameters $A(z) = C_2 LWC(z)$, leading to $\Omega = C_2 LWP$, and $B = 1$. Then, (5) becomes:

$$f_{r,z} = \left[1 - \frac{\beta}{\alpha} \Omega r^{-\beta} \right]^{1/\beta}. \quad (10)$$

The terminal velocity of droplets growing via ACC2 may be described by a power law that is close to the linear relation. Then, we can write $\beta = 1 + \delta$ with δ close to 0, leading to this approximate expression: $f_{r,z} \approx 1 - (1/\alpha)\Omega r^{-(1+\delta)}$. For $\delta \approx 0$, the modified spectrum is obtained by a translation of the initial spectrum that is size independent: $\Delta r \approx -(1/\alpha)\Omega$. The multiplication factor becomes $f_{r,z}^{2+\delta} \approx 1 - (2/\alpha)\Omega r^{-1}$, and represents the reduction of the concentration decreasing slowly with r increasing.

[24] During this stage of the accretional growth, the fact that the drizzle self-collection process is not taken into account may introduce some error, mainly for heavily drizzling cases.

3.2.2. Drizzle Evaporation

[25] The drizzle droplet evaporation process *EVP* below the cloud base is described for small droplets (smaller than about 30 to $50 \mu\text{m}$ radius) with negligible ventilation effect,

by the rate of size change that is inversely proportional to the size. However, for larger droplets, the value of the ventilation factor increases. For example, droplets with $r = 150 \mu\text{m}$ falling at 1.17 m s^{-1} near the ground have a ventilation factor around 2, depending slightly on the thermodynamical conditions (the droplet Reynolds number, Re , of around 23, introduced to the relation given by *Rogers and Yau* [1989]: $0.78 + 0.28Re^{1/2}$ gives ventilation factor slightly larger than 2). Here, the ventilation factor is taken as an approximate power law form ($f_{ven} = a_{ven}r^{b_{ven}}$ with $a_{ven} = 440m^{-0.6}$ and $b_{ven} = 0.6$) that underestimates a little the ventilation effect for $r < 30\text{--}40 \mu\text{m}$. The relation (2) for $PRC = EVP$ is then written as:

$$\left. \frac{dr}{dt} \right|_{EVP} \approx (S - 1)\xi_1 a_{ven} r^{-1+b_{ven}}, \quad (11)$$

where S is the saturation ratio, and ξ_1 is a function of temperature and pressure (given for example by *Rogers and Yau* [1989]). From the last relation, we can describe the evaporation process with $A(z) = [S(z) - 1]\xi_1(z)a_{ven}$, leading to $\Omega = a_{ven} \int_{z_0}^z [S(z) - 1]\xi_1(z) dz < 0$, and $B = -1 + b_{ven}$. For a drizzle spectrum composed of small droplets only, $a_{ven} = 1$ and $b_{ven} = 0$ have to be taken. The expression describing the function $f_{r,z}$ in (5) for evaporation is:

$$f_{r,z} = \left[1 - \frac{2 + \beta - b_{ven}}{\alpha} \Omega r^{-(2+\beta-b_{ven})} \right]^{1/(2+\beta-b_{ven})}. \quad (12)$$

For $\beta \approx 1$ and $b_{ven} \approx 0$, we have $f_{r,z} \approx [1 - (3/\alpha)\Omega r^{-3}]^{1/3} \approx 1 - (1/\alpha)\Omega r^{-3} > 1$ since $\Omega < 0$. Therefore, the initial spectrum would evolve by displacing toward the smaller sizes since $\Delta r \approx -(1/\alpha)\Omega r^{-2} > 0$ decreases rapidly with r increasing. The multiplication factor would be close to 1.

3.3. Doppler Spectrum Evolution Deduced From the Drizzle PSD Modifications Controlled by Microphysics

[26] Using a general power law relation (3) for V_f in the Rayleigh regime, the Doppler spectrum at a height z can be written as:

$$S(V_f, z) = S(r, z) = C^{te} n(r, z) f(r), \quad \text{with } f(r) = r^{7-\beta} / (\alpha \beta). \quad (13)$$

where the value of the constant C^{te} is a function of the used radar wavelength and the refractive index, and that can be dropped when discussing the Doppler spectrum [*Atlas et al.*, 1973]. Therefore, any moment of the Doppler spectrum is directly proportional to the PSD moment of order higher by $7 - \beta$. This means that the contribution to the Doppler spectrum of the larger droplets rapidly increases with size.

[27] Inside a cloud, $n(r, z)$ is composed of the cloud and drizzle modes. In this study, the part describing the drizzle mode is represented as a superposition of spectra injected progressively at different levels. The evolution of each of these distributions is calculated independently according to (4) starting from the injection level proper for each distribution. This evolution is based on the assumption that the selected unique power law relations for terminal velocity, and one of the two accretion rates or ventilation factor are valid for the whole distribution. Since these power laws are a good approximation over a limited range of droplet sizes

only, the contribution of the droplets that are outside of the corresponding subrange must be insignificant for the simulated layer. This imposes a limitation for the size domain of the initial PSDs and the vertical extension of the studied cloud layer.

[28] The cloud contribution to $n(r, z)$ in (13) is calculated assuming that the cloud droplets follow a lognormal distribution (given in (14) below) with a prescribed dispersion parameter σ (0.33) and total concentration N_{tot} , varying for maritime (100 cm^{-3}) and continental polluted clouds (500 cm^{-3}). The characteristic size r_0 is determined at each level from the cloud LWC profile which is prescribed in the form $LWC(z) = f_{ad} LWC_{ad}(z)$. The adiabaticity factor f_{ad} is calculated using the function proposed by *Chin et al.* [2000]. The cloud LWC and cloud droplet number concentration are also used to estimate the number concentration autoconversion rate [*Wood*, 2005], allowing the evaluation of the injected total number concentration of the initial distributions for each individual drizzle spectrum. The drizzle growth via accretion is expressed as a function of LWC only as given in (8a) and (8b).

[29] The predicted microphysical evolution of the total drizzle spectrum and the cloud droplet PSD are introduced in the simulator to calculate the expected Doppler velocity spectrum and its different moments.

[30] For a given simulated layer, the initial input drizzle PSDs are represented by a lognormal (e.g., as in work by *Frisch et al.* [1995]) or generalized gamma function:

$$n(r) = N_{tot} \left(\sqrt{2\pi} \right)^{-1} (\sigma r)^{-1} \exp \left\{ -0.5 [\ln(r/r_0)/\sigma]^2 \right\} \quad (14)$$

$$n(r) = N_{tot} \frac{\gamma}{\Gamma((\mu+1)/\gamma)} r_n^{-(\mu+1)} r^\mu \exp[-(r/r_n)^\gamma] \quad \text{or} \\ n(r) = N_0 r^\mu \exp[-(r/r_n)^\gamma] \quad (15)$$

The generalized gamma (GG) function includes, besides the three parameters describing the standard gamma distribution (total number concentration N_{tot} or intercept parameter N_0 , characteristic size r_n and shape parameter μ), an additional dispersion parameter γ that mainly controls the distribution of larger droplets, called the tail parameter [*Xie and Liu*, 2009]. The GG function has been used to describe the cloud droplet size distribution [e.g., *Tampieri and Tomasi*, 1976; *Lim and Hong*, 2010], raindrop PSD [e.g., *Szyrmer et al.*, 2005] and precipitating ice [e.g., *Delanoë et al.*, 2005].

[31] The choice of the PSD functional form (14 or 15) and the selected set of its parameters is the one that generates at the top level of the simulated layer all Doppler moments of interest (from reflectivity to kurtosis) close to the average observed values corresponding to the given conditions. Here, we want to show that starting with this distribution, the PSD evolution under a given microphysical process assuming appropriate environment, is close to the observed tendencies.

4. Modeling Results and Doppler Radar Observations

4.1. Early Drizzle Growth (Near Cloud Top)

[32] Taking a cloud layer near cloud top where the first drizzle precursors are generated by autoconversion, the

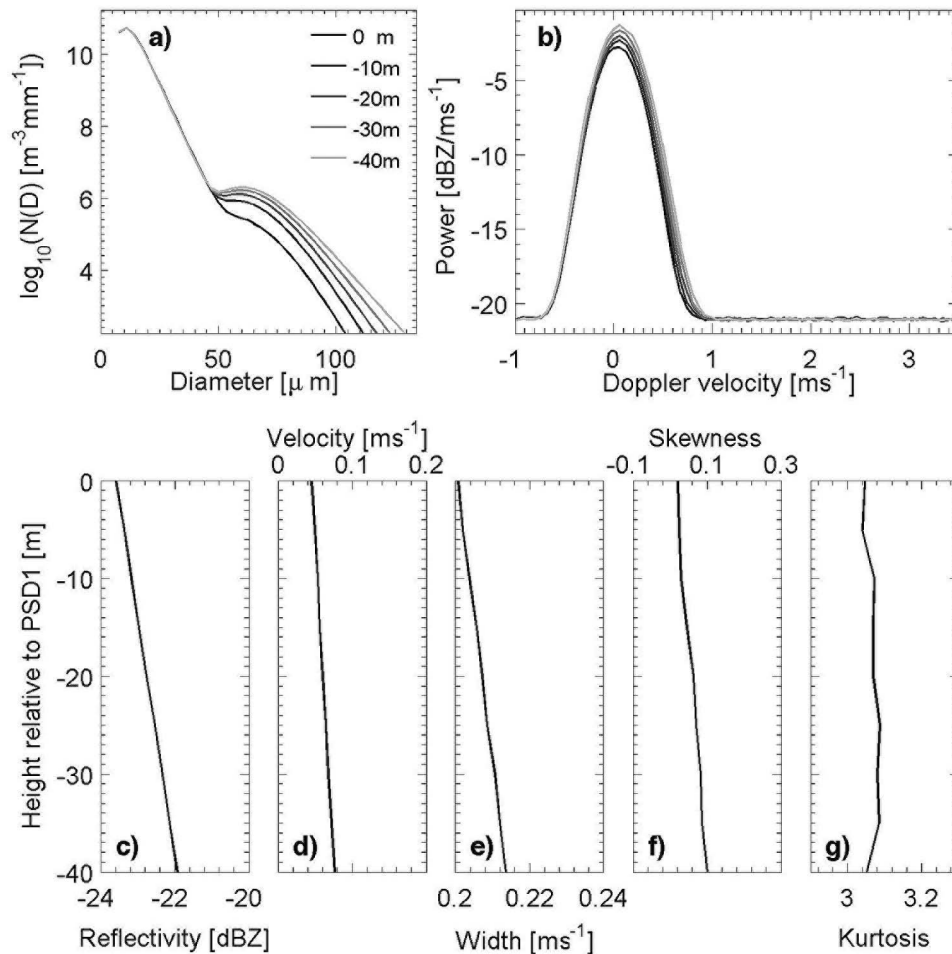


Figure 4. (a) Evolution of the continental PSDs near the cloud top, as modeled considering only the ACC1 process. (b) Simulated radar Doppler spectra corresponding to those PSDs, where no air motion and a turbulence width of 0.2 ms^{-1} were assumed. (c–g) Evolution of the five Doppler spectrum parameters, as computed by the simulator.

parameterization for ACC1 can be applied since we can assume the absence of larger droplets. A fallen distance of 40 m is considered sufficiently small to have not yet generated the larger droplets for which the kernel and velocity parameterizations are no longer valid. This growth represents the transition regime described in section 2, where the drizzle begins to affect the parameters of the Doppler spectrum. Starting from the uppermost level of the layer, a new distribution of droplets freshly transferred to the drizzle category is introduced every 5 m, and then evolves according to (4) with (9). The size distribution of freshly injected drizzle has a lognormal form with logarithmic width of 0.15 and geometric mean radius of $30 \mu\text{m}$. The total number concentration of the topmost drizzle PSD is equal to $5.3 \cdot 10^3 \text{ m}^{-3}$. The curves presented in Figure 4a show the total predicted droplet size distribution every 10 m. Each line represents the sum of the cloud distribution and superposition of all the drizzle spectra that are input above or at a given cloud level. As predicted by (4) given (9) for an individual spectrum, the changes are rather small for smaller drizzle droplets and increase progressively with r . This effect is amplified in the Doppler spectrum calculated by the simulator as shown in Figure 4b.

Figures 4c–4g present the vertical changes of the five Doppler spectrum parameters calculated by the simulator.

[33] This example has been obtained assuming continental cloud conditions and should then describe the average behavior observed around -24 to -22 dBZ for the continental cases shown in Figure 1. In fact, the results compare well for the first three parameters (velocity, width and skewness): in both the model and observations, they present a slow increase as the drizzle grows (i.e., as the reflectivity increases and the drizzle impact on the Doppler spectrum becomes more apparent). As for the kurtosis, no clear behavior can be drawn from either the observations or the simulations in that range of reflectivities. Nonetheless, an average value above three was found, which relates well with the observations.

4.2. Growth by Accretion of the Well-Developed Drizzle

[34] The presence of heavy drizzle in deep clouds (marked by reflectivity higher than about 0 dBZ) completely dominates the Doppler spectrum, and different tendencies with increasing reflectivity can be noticed for continental and maritime clouds as discussed in section 2. The Doppler

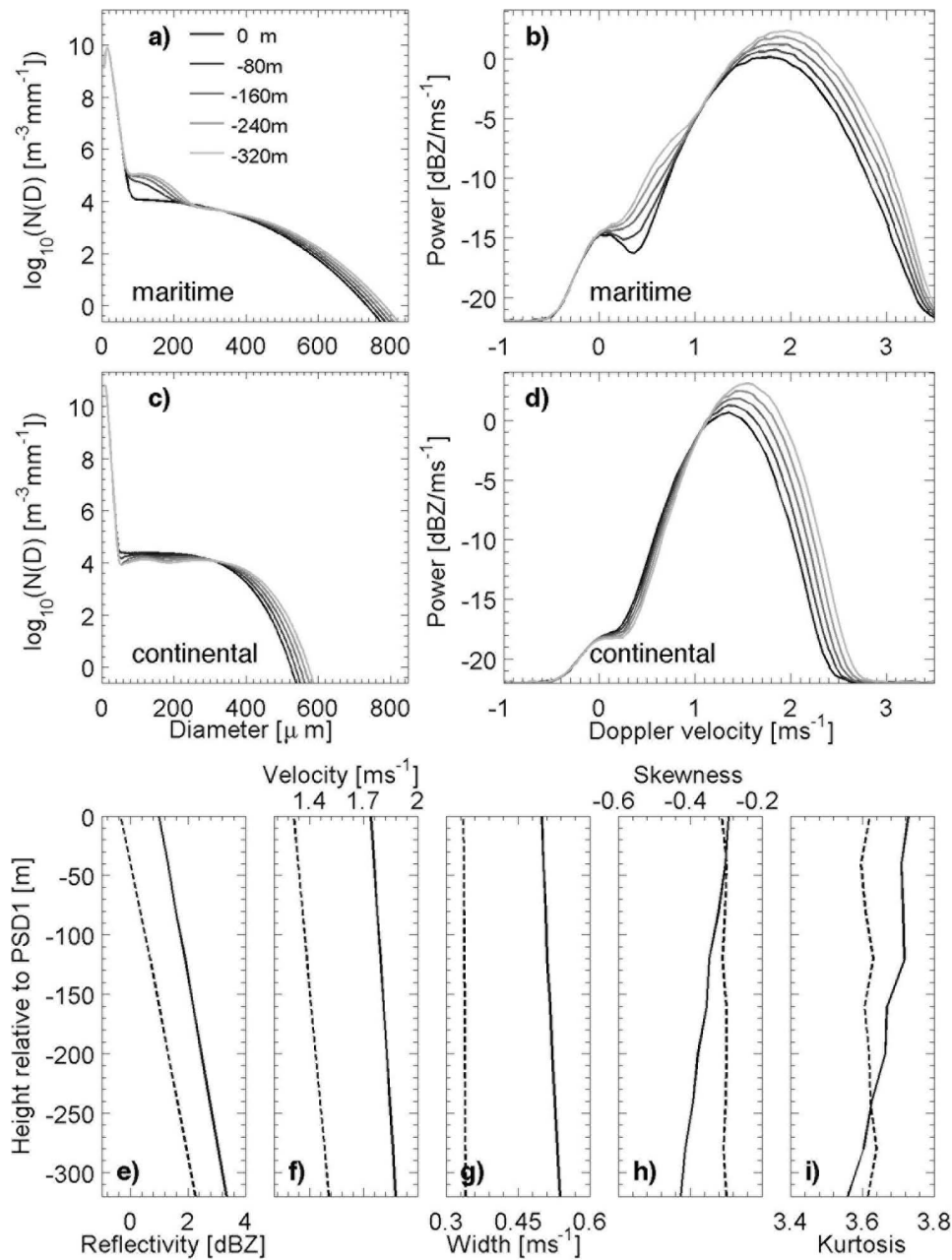


Figure 5. Evolution of the (a) maritime and (c) continental PSDs when drizzle is well developed in the cloud, as modeled considering only the *ACC2* process. (b, d) Simulated radar Doppler spectra corresponding to those PSDs, where no air motion and a turbulence width of 0.2 ms^{-1} were assumed. (e–i) Evolution of the five Doppler spectrum parameters, as computed by the simulator. The solid and dashed lines are for the maritime and continental PSDs, respectively.

velocity increases more rapidly in maritime than in continental clouds, with a spectrum broadening observed only in the maritime clouds. This broadening is even accompanied by the skewness becoming more negative, while it stays rather constant for the continental clouds. To have some insight into the microphysical causes of the observed differences, we perform the calculations of the spectra evolution within two clouds having the same constant LWC but with different droplet number concentrations: 100 cm^{-3} and 500 cm^{-3} for maritime and continental, respectively. In both

cases, the first drizzle PSD at the layer top produces similar reflectivity (just above 0 dBZ), but with slightly larger Doppler velocity and width in the maritime clouds to be in agreement with the climatology shown in Figure 1. In both cases, the PSD is described by a GG function with the same characteristic radius equal to $165 \mu\text{m}$ and the shape parameter $\mu = 0$. The difference in the spectra width is obtained by setting the tail parameter to 3 and 5 respectively for maritime and continental clouds. The value of the intercept parameter is $1.2 \cdot 10^7 \text{ m}^{-4}$ in maritime PSD, and

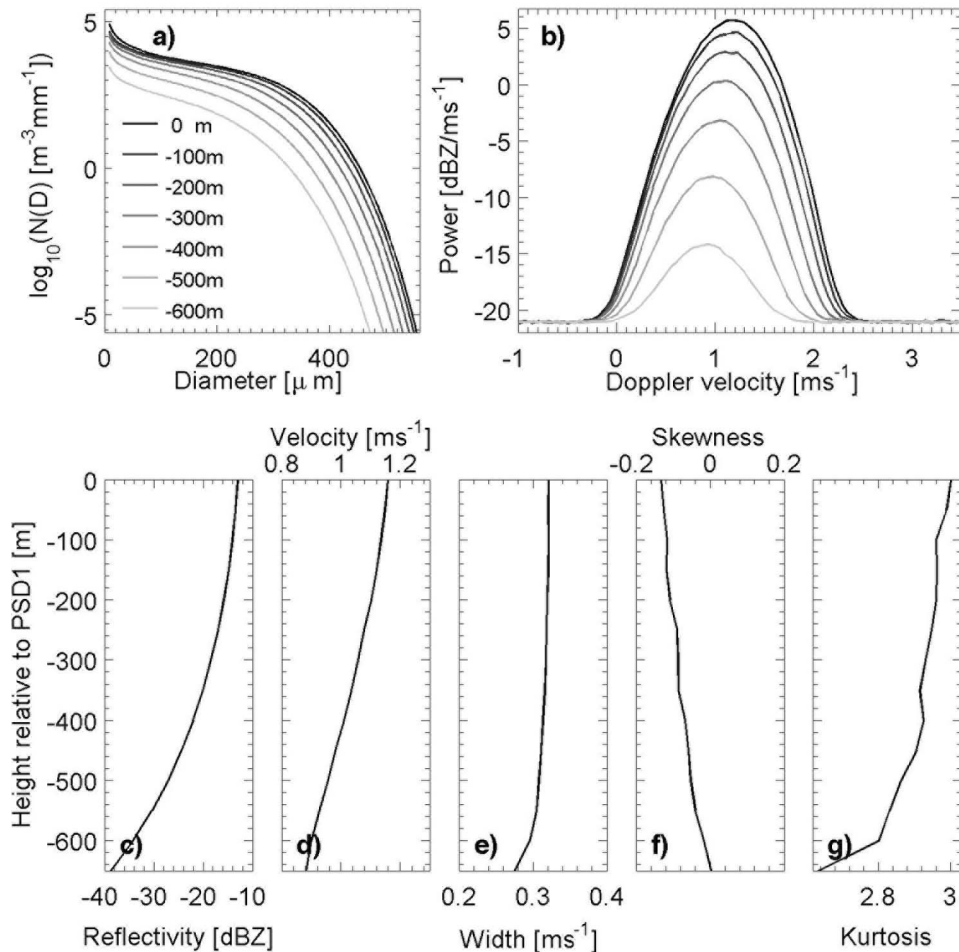


Figure 6. (a) Evolution of the drizzle PSDs below a cloud, as modeled considering only the *EVP* process. (b) Simulated radar Doppler spectra corresponding to those PSDs, where no air motion and a turbulence width of 0.2 ms^{-1} were assumed. (c–g) Evolution of the five Doppler spectrum parameters, as computed by the simulator.

$2.4 \cdot 10^7 \text{ m}^{-4}$ in continental PSD. Every 40 m, a new drizzle PSD is introduced. All the initial spectra are assumed to be already sufficiently developed to be described by the *ACC2* parameterization (their characteristic radius is set to 65 and $60 \text{ } \mu\text{m}$ respectively in maritime and continental case). This means that we neglect the contribution to the Doppler spectrum of the drizzle droplets newly generated just at and above a given level that evolves via *ACC1*. The results are shown in Figure 5. The main difference is in the intensity of the introduced PSDs within the simulated cloud layer: almost negligible in the continental case and much more important in the maritime. This difference results from the dependence of the autoconversion rate of the number concentration on the cloud droplet concentration prescribed for the two clouds. The growth of the PSD and the Doppler spectrum evolution at the larger droplet tail is very similar in the two cases since the accretional growth is mainly a function of the cloud LWC, and identical for both. However, the continuous addition to the initial spectrum of the new spectra due to the autoconversion still active in the maritime clouds, leads to a continuous increase of the total spectrum width and a skewness growing more negative, while these two parameters are constant throughout the continental

growth (see Figures 5g and 5h), as observed previously in Figure 1.

[35] Nevertheless, a more rapid increase of mean Doppler fall velocity with radar reflectivity in the maritime than in the continental clouds is not obtained. As discussed in section 2, this increase could be a consequence of the formation of larger droplets via the self-collection between drizzle droplets, not taken into account in the simulated PSD evolution. Using the proposed parameterization of self-collection [Beheng, 1994], the average rate of self-collection in our simulated maritime case is about $0.1 \text{ m}^{-3} \text{ s}^{-1}$. Assuming an average velocity of 1 m s^{-1} , a rough estimation then gives 10 collision events during 100 m distance fallen. The enhancement of the self-collection ratio can be from turbulence and also an increase of collision probability can be expected due to a rather wide PSD of drizzle in the maritime case.

4.3. Evaporation Below Cloud Base

[36] To model the drizzle Doppler spectrum below the cloud, we assume a column located at some small distance below the cloud base with only a drizzle PSD present at the column top. The imposed gradient of relative humidity is

0.36 km^{-1} corresponding to temperature of 15°C [Comstock *et al.*, 2004]. To choose the shape of the initial spectrum, we tried the lognormal and generalized gamma functions with different dispersion parameters. An important variability of the Doppler moments has been obtained depending on the choice of the parameter sets defining the size distribution. A variability of observed profiles below the cloud base can be also noticed in Figure 2. In Figure 6, we present the results obtained with the initial spectrum taken as a generalized gamma distribution with shape parameter -1 and the tail parameter equal to 5 , the characteristic radius is $150 \mu\text{m}$ and the value of 650 m^{-3} is taken as intercept parameter. The calculated evolution of the Doppler spectrum parameters, shown in Figures 6c–6g, represents some of the below cloud profiles observed in Figure 2.

[37] The vertical changes of the evaporating drizzle PSD as deduced from (4) with (12) are presented in Figure 6a. The modifications of the spectrum are similar to the evolution of the evaporating light rain PSD calculated by Li and Srivastava [2001]. The larger droplet tail stays almost parallel to its initial form. An upward tilt maintained for the smallest droplets is due to the rapid decrease of the terminal velocity with decreasing size, and therefore increase of their concentration from flux number conservation. In general, the effect of evaporation increases with the progressive shift of the PSD toward the smaller sizes.

5. Summary

[38] The recording of the full radar Doppler spectrum is now a common approach in profiling cloud radars, and is certainly the standard for all ARM profiling radars since 2004. The argument for recording the full radar Doppler spectrum, despite its impact on data volume, is our belief that the decomposition of the radar return as a function of observed Doppler velocities offers new opportunities for the study of cloud and precipitation microphysics and dynamics. This potential needs to be exploited systematically, especially in simple cloud systems such as liquid stratiform drizzling clouds. A proposed method for accomplishing this is through the careful use of radar Doppler spectra forward modeling and 1-D microphysical modeling. In part 1, new parameters that describe the radar Doppler spectrum were introduced and their application to remote sensing was discussed. Furthermore, the expected behavior of the radar observations in the transition regime from cloud-only to drizzling cloud observations was presented. It is important to note that the presence of nonlinear wind shear within the radar sampling volume can produce asymmetries (e.g., positive and negative skewness) in the radar Doppler spectra. This partially explains the observed variability of the radar Doppler moments seen in Figure 1. However, the dynamically induced asymmetries are short-lived and a 30 s low-pass filter of the high-resolution radar Doppler moments is sufficient to filter them out and only the lower-frequency microphysical signatures are maintained. In this study, comprehensive radar observations that reasonably agree with the expected behavior are presented. Furthermore, microphysical modeling coupled with a radar forward model is used to link observations with models, and address several noticeable features in the observations.

[39] A comprehensive comparison of continental and maritime radar observations was presented. The observed trends of the radar Doppler spectra moments as a function of radar reflectivity exhibit several similarities. However, a few noticeable differences were found and successfully explored using modeling. In the modeling study, representing drizzle PSDs within a cloud as a combination of individual spectra related to populations of droplets grown from cloud droplets into embryonic drizzle droplets at different in-cloud levels via two distinct regimes of accretional growth and terminal velocity are important simplifications. Our objective here is only to show the link between the microphysical processes and the observed pattern of the five radar Doppler spectrum parameters, rather than to try to model the drizzle microphysics, which would require a more advanced study of the relations and simplifying assumptions used. For example, the autoconversion as drizzle initiation process, an artifact of size distribution separation into two regimes, is subject to important uncertainty. The comparison of the autoconversion rate calculated using different proposed parameterizations shows very large discrepancy [e.g., Hsieh *et al.*, 2009]. Moreover, turbulence effects have to be included. That being said, the combination of microphysical modeling, forward modeling and observations successfully interprets observed differences between continental and maritime clouds.

[40] The transformation of the microphysical model output to radar Doppler spectrum and related radar observables (e.g., spectrum width and skewness) offers a methodology for interpreting radar observations and for improving microphysical modeling. This closed loop process offers new venues for examining cloud microphysics and dynamics at very small scales. The continuous recording of radar Doppler spectra from all the profiling cloud radars makes such observations widely available to the scientific community.

References

- Albrecht, B. A. (1989), Aerosols, cloud microphysics, and fractional cloudiness, *Science*, *245*, 1227–1230, doi:10.1126/science.245.4923.1227.
- Albrecht, B. A. (1993), Effects of precipitation on the thermodynamic structure of the trade wind boundary layer, *J. Geophys. Res.*, *98*, 7327–7337, doi:10.1029/93JD00027.
- Atlas, D., R. C. Srivastava, and R. S. Sekhon (1973), Doppler radar characteristics at vertical incidence, *Rev. Geophys.*, *11*, 1–35, doi:10.1029/RG011i001p00001.
- Beheng, K. D. (1994), A parameterization of warm microphysical conversion processes, *Atmos. Res.*, *33*, 193–206, doi:10.1016/0169-8095(94)90020-5.
- Chepfer, H., S. Bony, D. M. Winker, M. Chiriacco, J.-L. Dufresne, and G. Seze (2008), Use of CALIPSO lidar observations to evaluate the cloudiness simulated by a climate model, *Geophys. Res. Lett.*, *35*, L15704, doi:10.1029/2008GL034207.
- Chin, H.-N. S., D. J. Rodriguez, R. T. Cederwall, C. C. Chuang, A. S. Grossman, J. J. Yio, Q. Fu, and M. A. Miller (2000), A microphysical retrieval scheme for continental low-level stratiform clouds: Impacts of the subadiabatic character on microphysical properties and radiation budgets, *Mon. Weather Rev.*, *128*, 2511–2527, doi:10.1175/1520-0493(2000)128<2511:AMRSFC>2.0.CO;2.
- Comstock, K. K., R. Wood, S. E. Yuter, and C. S. Bretherton (2004), Reflectivity and rain rate in and below drizzling stratocumulus, *Q. J. R. Meteorol. Soc.*, *130*, 2891–2918, doi:10.1256/qj.03.187.
- Delanoë, J., A. Protat, J. Testud, D. Bouniol, A. J. Heymsfield, A. Bansemir, P. R. A. Brown, and R. M. Forbes (2005), Statistical properties of the normalized ice particle size distribution, *J. Geophys. Res.*, *110*, D10201, doi:10.1029/2004JD005405.
- Frisch, A. S., C. W. Fairall, and J. B. Snider (1995), Measurement of stratus cloud and drizzle parameters in ASTEX with a K_a -band Doppler radar and a microwave radiometer, *J. Atmos. Sci.*, *52*, 2788–2799, doi:10.1175/1520-0469(1995)052<2788:MOSCAD>2.0.CO;2.

- Gossard, E. E., R. G. Strauch, and R. R. Rogers (1990), Evolution of cloud drop-size distributions observed by ground-based Doppler radar, *J. Atmos. Oceanic Technol.*, *7*, 815–828, doi:10.1175/1520-0426(1990)007<0815: EODDIL>2.0.CO;2.
- Haynes, J. M., R. T. Marchand, Z. Luo, A. Bodas-Salcedo, and G. L. Stephens (2007), A multi-purpose radar simulation package: QuickBeam, *Bull. Am. Meteorol. Soc.*, *88*, 1723–1727, doi:10.1175/BAMS-88-11-1723.
- Hsieh, W. C., H. Jonsson, L.-P. Wang, G. Buzorius, R. C. Flagan, J. H. Seinfeld, and A. Nenes (2009), On the representation of droplet coalescence and autoconversion: Evaluation using ambient cloud droplet size distributions, *J. Geophys. Res.*, *114*, D07201, doi:10.1029/2008JD010502.
- Khairoutdinov, M. F., and Y. L. Kogan (1999), A Large eddy simulation model with explicit microphysics: Validation against aircraft observations of a stratocumulus-topped boundary layer, *J. Atmos. Sci.*, *56*, 2115–2131, doi:10.1175/1520-0469(1999)056<2115:ALESMW>2.0.CO;2.
- Klein, S. A., and C. Jakob (1999), Validation and sensitivities of frontal clouds simulated by the ECMWF model, *Mon. Weather Rev.*, *127*, 2514–2531, doi:10.1175/1520-0493(1999)127<2514:VASOFC>2.0.CO;2.
- Kogan, Y. L., M. P. Khairoutdinov, D. K. Lilly, Z. N. Kogan, and Q. Liu (1995), Modeling of stratocumulus cloud layers in a large-eddy simulation model with explicit microphysics, *J. Atmos. Sci.*, *52*, 2923–2940, doi:10.1175/1520-0469(1995)052<2923:MOSCLI>2.0.CO;2.
- Kollias, P., and B. A. Albrecht (2000), The turbulence structure in a continental stratocumulus cloud from millimeter wavelength radar observations, *J. Atmos. Sci.*, *57*, 2417–2434, doi:10.1175/1520-0469(2000)057<2417:TTSIAC>2.0.CO;2.
- Kollias, P., J. Remillard, E. Luke, and W. Szyrmer (2011), Cloud radar Doppler spectra in drizzling stratiform clouds: 1. Forward modeling and applications, *J. Geophys. Res.*, *116*, D13201, doi:10.1029/2010JD015237.
- Lenderink, G., and A. P. Siebesma (2004), On the role of drizzle in stratocumulus and its implications for large-eddy simulation, *Q. J. R. Meteorol. Soc.*, *130*, 3429–3434, doi:10.1256/qj.03.142.
- Li, X., and R. C. Srivastava (2001), An analytical solution for raindrop evaporation and its application to radar rainfall measurements, *J. Appl. Meteorol.*, *40*, 1607–1616, doi:10.1175/1520-0450(2001)040<1607: AASFRE>2.0.CO;2.
- Lim, K.-S. S., and S.-Y. Hong (2010), Development of an effective double-moment cloud microphysics scheme with prognostic cloud condensation nuclei (CCN) for weather and climate models, *Mon. Weather Rev.*, *138*, 1587–1612, doi:10.1175/2009MWR2968.1.
- Liu, Y., B. Geerts, M. Miller, P. Daum, and R. McGraw (2008), Threshold radar reflectivity for drizzling clouds, *Geophys. Res. Lett.*, *35*, L03807, doi:10.1029/2007GL031201.
- Long, A. B. (1974), Solutions to droplet collection equation for polynomial kernels, *J. Atmos. Sci.*, *31*, 1040–1052, doi:10.1175/1520-0469(1974)031<1040:STTDCE>2.0.CO;2.
- Miller, M. A., M. P. Jensen, and E. E. Clothiaux (1998), Diurnal cloud and thermodynamic variations in the stratocumulus transition regime: A case study using in situ and remote sensors, *J. Atmos. Sci.*, *55*, 2294–2310, doi:10.1175/1520-0469(1998)055<2294:DCATVI>2.0.CO;2.
- Rogers, R. R., and M. K. Yau (1989), *A Short Course in Cloud Physics*, 3rd ed., 290 pp., Elsevier, New York.
- Rogers, R. R., I. I. Zawadzki, and E. E. Gossard (1991), Variation with altitude of the drop-size distribution in steady light rain, *Q. J. R. Meteorol. Soc.*, *117*, 1341–1369, doi:10.1002/qj.49711750211.
- Saleeby, S. M., and W. R. Cotton (2004), A large-droplet mode and prognostic number concentration of cloud droplets in the Colorado State Univ. Regional Atmospheric Modeling System (RAMS). Part I: Module descriptions and supercell test simulations, *J. Appl. Meteorol.*, *43*, 182–195, doi:10.1175/1520-0450(2004)043<0182:ALMAPN>2.0.CO;2.
- Stevens, B., W. R. Cotton, G. Feingold, and C.-H. Moeng (1998), Large-eddy simulations of strongly precipitating, shallow, stratocumulus-topped boundary layers, *J. Atmos. Sci.*, *55*, 3616–3638, doi:10.1175/1520-0469(1998)055<3616:LESOSP>2.0.CO;2.
- Stevens, B., et al. (2003), Dynamics and chemistry of maritime stratocumulus—DYCOMS-II, *Bull. Am. Meteorol. Soc.*, *84*, 579–593, doi:10.1175/BAMS-84-5-579.
- Szyrmer, W., S. Laroche, and I. Zawadzki (2005), A microphysical bulk formulation based on scaling normalization of the particle size distribution. Part I: Description, *J. Atmos. Sci.*, *62*, 4206–4221, doi:10.1175/JAS3620.1.
- Tampieri, F., and C. Tomasi (1976), Size distribution models of fog and cloud droplets in terms of the modified gamma function, *Tellus*, *28*, 333–347, doi:10.1111/j.2153-3490.1976.tb00682.x.
- Wood, R. (2005), Drizzle in stratiform boundary layer clouds. Part II: Microphysical aspects, *J. Atmos. Sci.*, *62*, 3034–3050, doi:10.1175/JAS3530.1.
- Xie, X., and X. Liu (2009), Analytical three-moment autoconversion parameterization based on generalized gamma distribution, *J. Geophys. Res.*, *114*, D17201, doi:10.1029/2008JD011633.

P. Kollias, J. Rémillard, and W. Szyrmer, Department of Atmospheric and Oceanic Sciences, McGill University, Burnside Hall, Rm. 945, 805 Sherbrooke St. W., Montreal, QC H3A 2K6, Canada. (pavlos.kollias@mcgill.ca)

E. Luke, Atmospheric Sciences Division, Brookhaven National Laboratory, Bldg. 490D, Bell Avenue, Upton, NY 11973, USA.